05

Effects of thermomagnetic prehistory in the behavior of magnetization of a powder system of synthetic nanoferrihydrite in the presence of magnetic interparticle interactions

© D.A. Balaev[1], A.A. Krasikov[1], S.V. Stolyar[1,2], R.N. Yaroslavtsev[1,2], S.A. Skorobogatov[1], D.A. Velikanov[1], R.S. Iskhakov[1]

[1] Kirensky Institute of Physics, Federal Research Center KSC SB, Russian Academy of Sciences, Krasnoyarsk, Russia
[2] Krasnoyarsk Scientific Center of the Siberian Branch of the Russian Academy of Sciences, Krasnoyarsk, Russia

E-mail: dabalaev@iph.krasn.ru

Received October 18, 2024
Revised October 28, 2024
Accepted October 29, 2024

The temperature dependences of the magnetization $M(T)$ of two powder systems of ferrihydrite nanoparticles with identical sizes of ferrihydrite particles (average particle size is ≈ 2.7 nm) and different intensities of magnetic interparticle interactions (MII) were studied. In addition to the commonly observed increase in the superparamagnetic blocking temperature T_B (from 17 K to 50 K), MIIs clearly manifest themselves under different conditions and regimes of thermomagnetic prehistory. It was found that the rate of pre-cooling in an external magnetic field (in the used range of 1–10 K/min) affects the magnitude of the magnetization of the system at low temperatures and the shape of the $M(T)$ dependence in the temperature range up to T_B. This effect is significant for fairly weak external fields (up to ~ 300 Oe), and when the field increases to ~ 800 Oe, the cooling rate becomes insignificant for the magnitude of magnetization. In this case, for the range of external fields up to ~ 300 Oe, the $M(T)$ dependences obtained during cooling in an external field and when heating the sample in the field (after pre-cooling) are different. For a system of ferrihydrite nanoparticles, in which the MIIs are weakened, these effects are absent. Analysis of the results obtained allowed us to propose the following scenario for the implementation of the detected thermomagnetic effects. In the presence of MIIs (in the temperature range below T_B), the basic state of the structure of the magnetic moments of particles μ_P is such that the vectors μ_P of neighboring particles tend to be oriented predominantly against each other (anticollinearly). This takes place upon relatively „slow“ cooling of the system (1 K/min), but upon „fast“ cooling (10 K/min), i. e. „hardening“ in an external field, the μ_P vectors remain predominantly directed „along the field“ as in the temperature region of the superparamagnetic state (at $T > T_B$). The range of magnetic fields in which the described effects are observed is determined by the competition between the MII energy and the Zeeman energy $\mu_P \cdot H$.

Keywords: nanoferrihydrite, magnetic interparticle interactions, magnetization.

DOI: 10.61011/PSS.2024.11.60092.284

1. Introduction

The relevance of study of ensembles of magnetic nanoparticles is attributable to the possibility of their practical use (for example, in biomedicine, in environmental applications) [1–3], as well as the fundamental component — the need to identify the manifestations of surface and size effects in the magnetic properties of nanoparticles [4–9]. In addition to these effects (associated with a large proportion of surface atoms) inherent in individual nanoparticles, magnetic interparticle interactions (MII) also play an important role in the magnetic properties of nanoparticle ensembles [10–13]. One of the most well-known manifestations of MII is an increase of the temperature of superparamagnetic (SPM) blocking of systems of interacting particles compared to such systems in which particles of the same size are spatially separated from each other [14–22]. The MII in the nanoparticle system can affect the type of the magnetization curve and the value of the coercive force [23,24]. Undoubtedly, the presence of MII also affects such an important characteristic in biomedical applications (hyperthermia) as the heating rate when applying an alternating magnetic field [25].

Various states of the magnetic moments of the particles can be realized in ensembles of nanoparticles depending on the intensity of the MII, which can be regulated by the distance between the particles and the magnitude of their magnetic moments μ_P [26,27]. The transition (with a decrease of temperature) from the SPM state to the blocked state of the magnetic moments of particles is accompanied in all cases by an increase of the reversal time τ of the vector μ_P. The value τ is determined by the competition of thermal energy and magnetic anisotropy energy for non-interacting particles, according to the Boltzmann distribution. However, the value τ increases faster with a decrease of temperature in case of sufficiently strong MII, and collective processes

of freezing of the magnetic moments of particles should be discussed. An analogy to the well-known transition to the spin glass state is appropriate here, but instead of the spin of an atom, we mean „superspin", i.e., μ_P. And finally, we can expect the ordering of „superspins" for highly filled systems (with maximum volume concentration), i.e., the realization of the so-called „superferromagnetic" state [26].

It is most logical to consider dipole-dipole interactions as a source of MII. However, the realization of magnetic interaction through exchange bonds between the surface atoms of neighboring particles is not excluded for concentrated systems [10,28,29]. Of course, each nanoparticle system has its own characteristics, consisting in the properties of the particle surface, the defects in their structure, and the size of μ_P.

We will discuss the manifestation of MII in nanoferrihydrite powder systems in this paper.[1] The magnetic moments of iron atoms in ferrihydrite are antiferromagnetically ordered [30], but a sufficiently significant uncompensated magnetic moment is formed due to structural defects in nanoparticles of antiferromagnetically ordered materials. For example, the value μ_P for ferrihydrite particles with size of 3–5 nm reaches several hundred Bohr magnetons [31–40]. Therefore, the magnetic behavior of antiferromagnetic (AFM) nanoparticles is similar to that of ferro- and ferrimagnetic nanoparticles. The impact of MII on the magnetic properties of powder systems of AFM nanoparticles has been established in a number of studies [10,21,22,41–52], including studies of ferrihydrite [21,22,45–52]. It was found for ferrihydrite that the rate of deceleration of the characteristic time τ with the decrease of temperature obeys the scaling law characteristic of the „superspin" glass type [48–50]. At the same time, the observed increase of the transition temperature to the SPM state for ferrihydrite without additional coating of nanoparticles due to MII significantly exceeds the estimate of the contribution of the energy of magnetic dipole-dipole interactions in this system [50–52]. The analysis of the dependence of the blocking SPM temperature on the external field within the framework of the model [53] showed the possibility of realizing the correlated behavior of the magnetic moments of particles in a certain volume (cluster). The effective size of such a cluster decreases with the growth of the external field [51,52]. Consequently, the source of MII in ferrihydrite powder systems can be indirect exchange (or superexchange) interactions between the surface atoms of neighboring particles.

The impact of the cooling rate in an external field on the state of magnetization was studied in this work for further examination of the manifestation of MII in the magnetic properties of ferrihydrite powder systems, as well as for determining the MII mechanism. Two representative samples that were characterized earlier [49,50,52] were taken for this purpose. Ferrihydrite nanoparticles are in close contact with each other in one sample, and the MII effect is maximal, while nanoparticles (of identical sizes) are coated with a layer of arabinogalactan polysaccharide in the other sample, which ensures suppression of MII.

[1] Ferrihydrite mineral with nominal chemical formula of $5Fe_2O_3 \cdot 9H_2O$ exists only in nanoscale form.

2. Experiment

2.1. Preparation and results of characterization of samples

The procedure for obtaining samples of synthetic ferrihydrite with addition of various amounts of arabinogalactane (AG) was described in detail earlier; AG was added at one of the stages of obtaining ferrihydrite [52]. Two samples were studied: the initial ferrihydrite without the addition of AG (hereinafter — FH-uncoated), and ferrihydrite with a mass concentration of AG of about 50% (hereinafter — FH-coated). The technological procedure implies the identical size of individual ferrihydrite nanoparticles in the FH-uncoated and FH-coated samples.

It was found using the transmission electron microscopy data that the average particle size of ferrihydrite without organic coating was 2.7 nm, and this value coincides well with the estimate according to the Scherrer formula obtained from the half-width of the first (brightest) diffraction ring from the micro-difraction pattern [50].

The changes of Fe $2p$, O $1s$ and C $1s$ spectra of the studied samples according to X-ray photoelectron spectroscopy data indicate the formation of an organic coating of ferrihydrite nanoparticles in the FH-coated sample, and no significant changes of the states of the particles themselves are observed [52].

The identical properties of individual ferrihydrite particles in the FH-uncoated and FH-coated samples are also indicated by the results of the analysis of the Mossbauer spectra, which are described by the same parameters for all samples responsible for the three unequal iron positions characteristic of ferrihydrite (with quadrupole splitting characteristic of each position) [52].

2.2. Measurements of magnetic properties

The temperature dependences of magnetization $M(T)$ were measured using three installations: the original SQUID magnetometer [54] (used to perform measurements of $M(T)$ in an external field of 50 Oe), the original vibrating sample magnetometer [55] (measurements of $M(T)$ were performed in external fields of 100 Oe and higher) and commercial vibrating sample magnetometer of PPMS-9 facility (Quantum Design). The sample was securely fixed in a measuring capsule. The magnetization data is given in units of emu, reduced to the mass of the sample (excluding AG). The cooling rate in the external field was ≈ 10 K/min for the first two installations, the cooling rate of PPMS-9 was ≈ 1 K/min. The heating rate of the sample was 1 K/min for all three magnetometers.

The measurements were conducted in three modes of thermomagnetic history:

(1) ZFC (zero field cooled) mode — measurement of dependence $M_{ZFC}(T)$ when the sample is heated in an external field after cooling in a zero external field;

(2) FCC (field cooled cooling) mode — measurement of the dependence $M_{FCC}(T)$ in case of cooling of the sample in an external field from the temperature exceeding the temperature of the SPM blocking, and the cooling rate for this mode was ≈ 1 K/min;

(3) FCW (field cooled warming) mode — measurement of the dependence $M_{FCC}(T)$ when the sample was heated in an external field after cooling in an external field of the same magnitude, and the pre-cooling rate for this mode was either 1 K/min, or 10 K/min.

3. Results and discussion

The main results illustrating the effect of the pre-cooling rate in an external field and the effect of thermomagnetic history on magnetization are shown in Figure 1 (FH-uncoated sample) and Figure 2 (FH-coated). The typical behavior of magnetization for ensembles of single-domain magnetic particles during the transition from the SPM state to the unblocked state can be seen from the presented data (see the curves of both figures), which is accompanied by a distinct peak of the dependence $M_{ZFC}(T)$ (hereinafter we denote the temperature of the peak of dependence $M_{ZFC}(T)$ as T_B) and the impact of thermomagnetic history (ZFC, FCW modes) on magnetization in the region $T < T_B$. It should be noted that the field range for the data in Figure 1 and 2 is quite small (50−800 Oe and 50−300 Oe, respectively), and a significant shift of temperature T_B to the low temperature range with an increase of the external field characteristic of SPM systems is observed in fields greater than ~ 1 kOe [50,52].

The following cardinal differences can be identified from a comparison of the behavior of the curves shown in Figures 1 and 2. First of all, it can be seen that the value T_B is noticeably less than for an FH-uncoated sample for a sample with FH-coated particles (with weakened magnetic interactions). Given the identity of the sizes and magnetic properties of the individual particles in these samples, it is natural to associate the large value T_B for the FH-uncoated sample with the influence of MII. However, the most important difference for the purposes of this work is the difference between the impact of thermomagnetic history and the cooling rate in the field on the relative magnitude of magnetization at low temperature, as well as on the dependences $M_{FCC}(T)$ and $M_{FCW}(T)$ of these samples. The following features can be identified for the FH-uncoated sample:

(i) the difference between dependencies $M_{FCW}(T)$ after „fast“ (10 K/min is indicated below as $M_{FCW\_10K/min}$), or „slow“ (1 K/min is indicated below as $M_{FCW\_1K/min}$) pre-cooling;

(ii) the visible difference between the dependencies $M_{FCC}(T)$ and $M_{FCW}(T)$ for „slow“ cooling (1 K/min).

It can be concluded from the analysis of the experimental curves in Figure 1 that the features (i) and (ii) are best manifested in weak fields ($H = 50$, 150 and 300 Oe — Figure 1, *a, b, c* respectively). The dependences $M_{FCC}(T)$ (in case of slow cooling) and $M_{FCW}(T)$ practically coincide with the increase of the external field to 800 Oe, and the effect of the pre-cooling rate on the dependence $M_{FCW}(T)$ becomes insignificant, see Figure 1, *d*. Thus, the following inequalities occur in the range of weak fields for the FH-uncoated sample (with strong MII) at $T < T_B$:

$$M_{FCC} > M_{FCW}, \tag{1a}$$

$$M_{FCW\_10K/min} > M_{FCW\_1K/min}. \tag{1b}$$

A different pattern is observed for a sample with weakened MII (FH-coated), see Figure 2. It can be seen that there is no difference in the behavior and shape of the dependencies $M_{FCW}(T)$ in the conditions of „fast“ (10 K/min) or „slow“ (1 K/min) cooling. The same can be said about the dependencies $M_{FCC}(T)$ and $M_{FCW}(T)$, i. e., there are the following equalities within the limits of experimental accuracy instead of inequalities (1): $M_{FCC} = M_{FCW}$, $M_{FCW\_10K/min} = M_{FCW\_1K/min}$.

Reduction of the magnetization of the FH-uncoated sample in case of „slow“ cooling (inequality (1*b*)) This means that the processes of reorientation of the magnetic moments of the particles μ_P occur during cooling. However, the magnetization remains approximately at the same level after „fast“ cooling as at the temperature T_B, and the values of $M_{FCW\_10K/min}$ and $M_{FCW\_1K/min}$ at low temperatures differ quite significantly (for example, in fields 50 and 150 Oe — almost twice, see Figure 1, *a, b*). Therefore, the reorientation of vectors μ_P in case of „slow“ cooling can be described as a fairly fast process. The difference between the dependences $M_{FCC}(T)$ and $M_{FCW}(T)$, which is visible in Figure 1, *a, b, c*, is also related to the reorientation of the magnetic moments of particles during slow cooling.

Systems of ferrihydrite nanoparticles, including the samples studied in this paper[2], demonstrate the hysteresis of the magnetization curves [21,22,30,32,56,57] at $T < T_B$, and consequently, relaxation of the magnetization can always be observed under fixed external conditions (at $T = \text{const}$, $H = \text{const}$). Usually, the relaxation of magnetization is studied after application/removal of an external field of a sufficiently large magnitude, or after cooling in sufficiently large fields [29,56–58]. The change of magnetization in such processes is associated with the overcoming by magnetic moments μ_P of barriers caused by magnetic anisotropy attributable to thermal fluctuations. And usually the change (relaxation) of the magnetization does not exceed several percent during a reasonable observation time $\sim 10^{3-4}$ s [29,56–58]. Consequently, rather rapid processes of magnetization relaxation observed from the data analysis

[2] The value of the coercive force for the FH-uncoated and FH-coated samples at $T = 4.2$ K is ≈ 4.0 and ≈ 1.8 kOe, respectively [50]

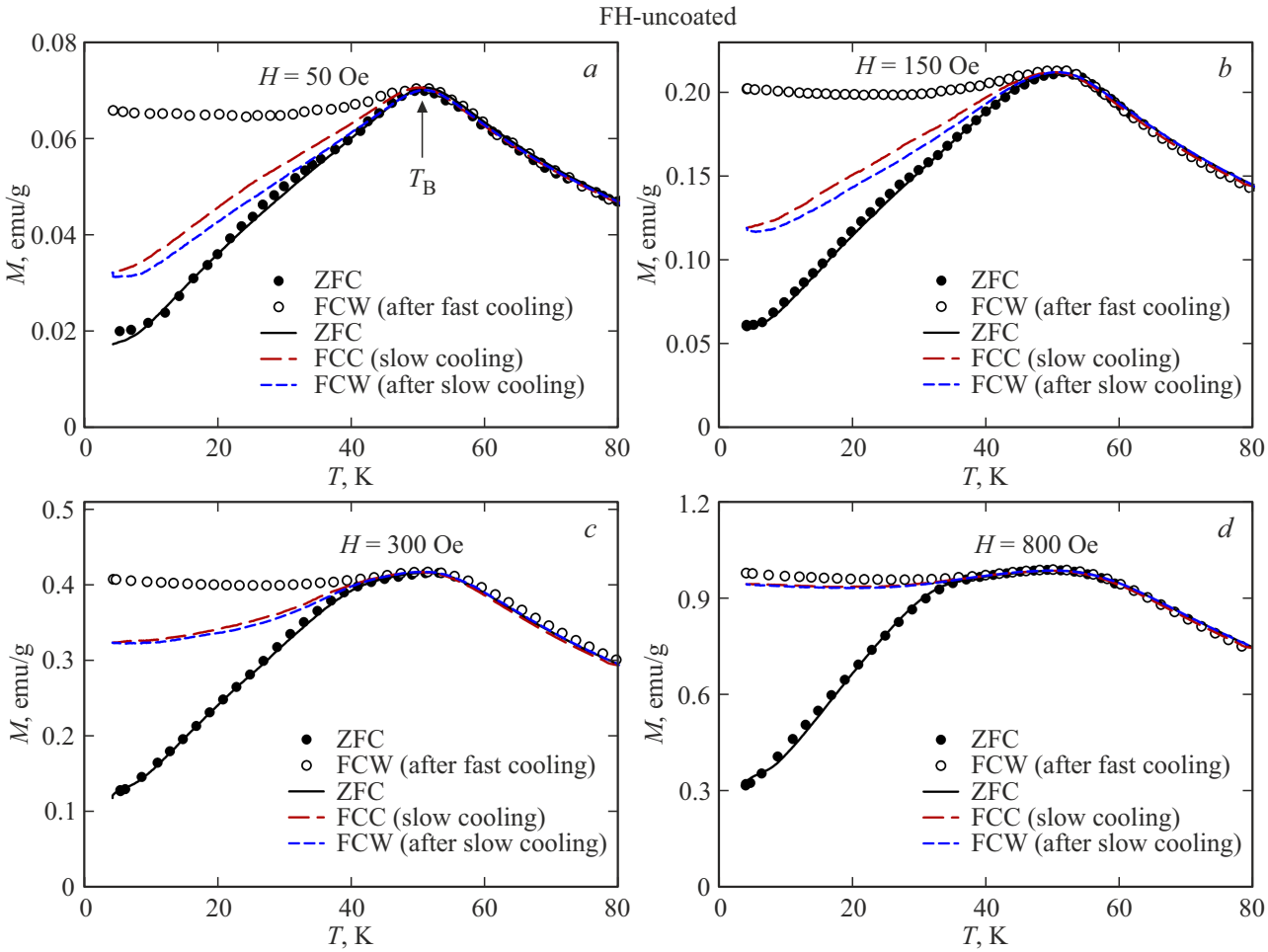

Figure 1. Temperature dependences of the magnetization of the FH-uncoated sample at different thermomagnetic history and after different cooling rates in an external magnetic field, see Section 2 and the legend; the values of the external field are indicated in the field of figures, the temperature of the peak of dependence $M_{ZFC}(T)$ — T_B is indicated on (a).

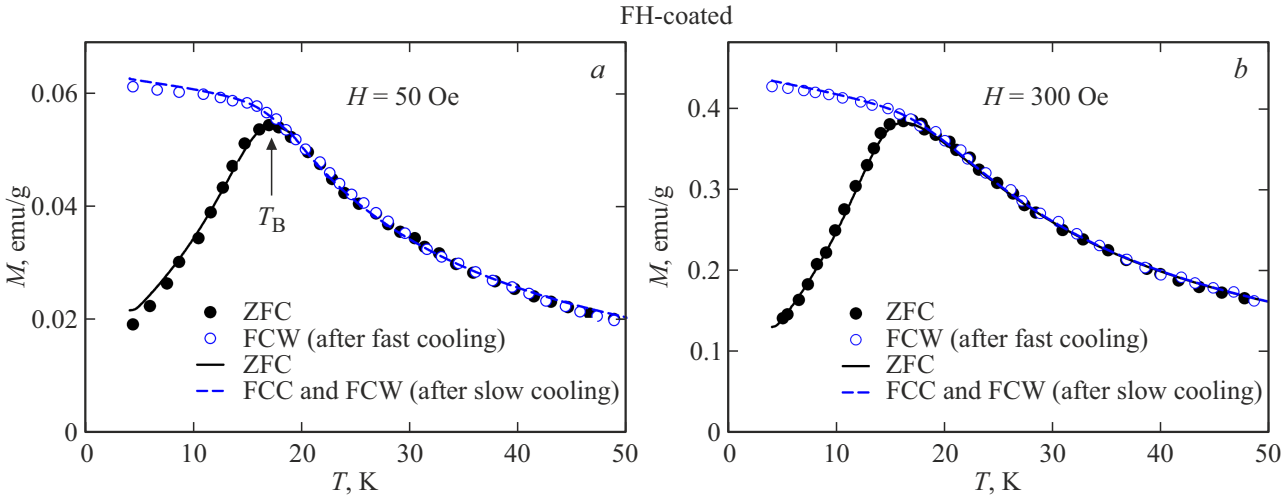

Figure 2. The temperature dependences of the magnetization of an FH-coated sample at different thermomagnetic history and after different cooling rates in an external field, see Section 2 and the legend; the values of the external field are indicated in the field of figures, the maximum temperature of the dependence $M_{ZFC}(T) - T_B$ is indicated on (a).

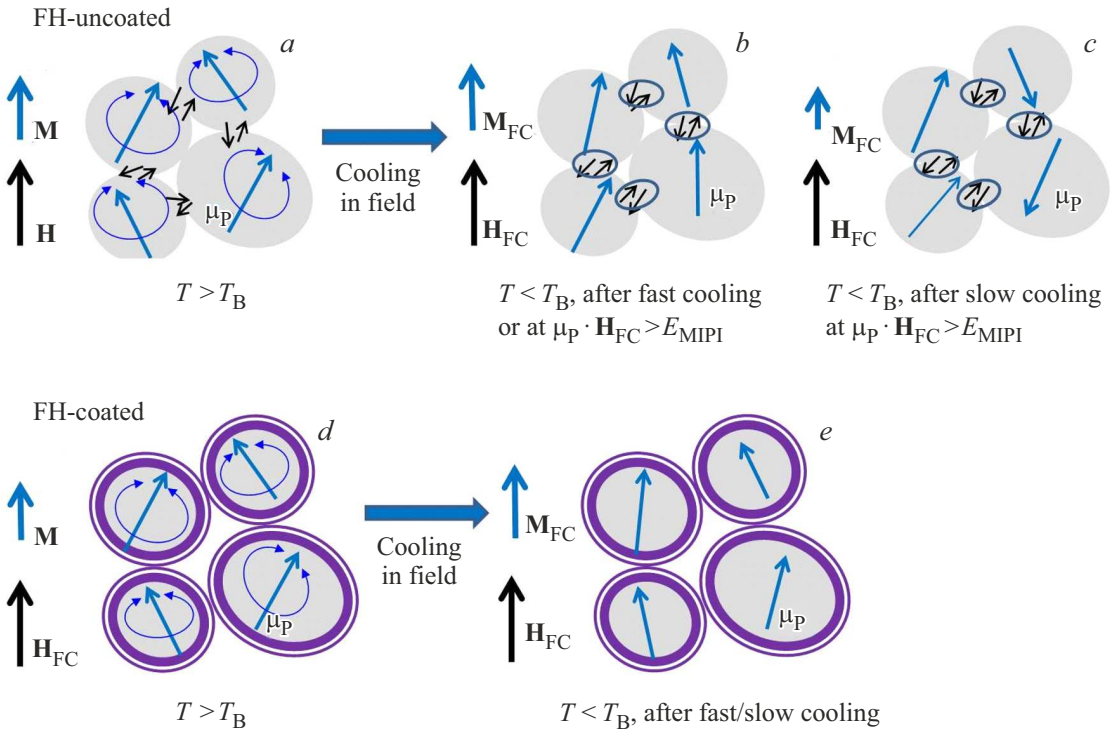

Figure 3. Schematic representation of the configuration of the external field vectors H, the magnetic moments of the particles μ_P (long arrows) and the magnetization M for FH-uncoated samples — (*a*), (*b*), (*c*) and FH-coated samples — (*d*), (*e*). Ovals — ferrihydrite nanoparticles, the particles are surrounded by a shell for the FH-coated sample. The experimental conditions, namely, temperature ($T < T_B$, $T > T_B$), relative cooling rate, the ratio between the Zeeman energy $\mu_P \cdot H$ and the energy characteristic of MII — E_{MII}, are indicated in the field of figures. Small arrows — the spins of the surface iron atoms, the AFM type of their arrangement ensures the MII for the FH-uncoated sample.

in Figure 1 are determined by another mechanism. It is logical to assume that this mechanism is related to MII, since the role of MII is small for the FH-coated sample, and the impact of the cooling rate on the magnetization is not observed.

Let us turn to experiments on nanoparticle systems with strong MII, in which, the sample is exposed for a certain time to a certain temperature T^* ($T^* < T_B$) during cooling in a small external field [27,59–62]. In this case, a fairly rapid decrease of the magnetization can be observed at $T^* = \text{const}$ [59–61]. The dependence $M_{FCW}(T)$ exhibits an anomaly in the vicinity of the temperature T^* for this measurement protocol after the temperature is decreased and then increased (also in the external field), i. e., the so-called „memory effect“ takes place. The approach we used, namely the different cooling rates in the external field, is largely similar to the described measurement protocol.

The vectors of the magnetic moments of the particles μ_P have predominant directions along the external field H in the SPM state ($T > T_B$). The magnetization of the FH-uncoated sample after rapid cooling in a magnetic field remains approximately at the same level as at temperature T_B (see Figure 1). Apparently, the magnetic moments μ_P do not have time with such „quenching“ (10 K/min) in an external field to significantly change their direction relative to the state in which they were at the temperature $T > T_B$. Then, the dependence $M_{FCW}(T)$ weakly depends on temperature in case of slow heating (1 K/min), although it demonstrates a non-monotonic behavior (Figure 1). However, slow cooling leads to a significant (and monotonous) decrease of magnetization, see dependences $M_{FCC}(T)$ in Figure 1. This means that the configuration of the directions of the magnetic moments, which was above the temperature T_B, becomes energetically disadvantageous with slow cooling. In other words, the fulfillment of the inequality (1*b*) indirectly indicates that the vectors μ_P tend to form a „antiferromagnetically similar“ structure as a result of MII in the FH-uncoated sample.

The described scenario for the FH-uncoated sample is schematically shown in Figure 3, *a, b, c*, which shows the relative position of the vectors μ_P, H, as well as the total magnetization of the sample M_{FC} with approximately preserved magnetization M_{FC}. Figure 3, *a, b, c* schematically illustrates the type of MII mechanism for synthetic ferrihydrite, namely, the presence of exchange (direct or indirect) interactions between atoms of neighboring particles. The bonds through the exchange interactions of the surface atoms of neighboring particles are shown in Figure 3, *b, c* as pairs of antiferromagnetically ordered spins taking into account the AFM nature of the interactions of the magnetic moments of iron in ferrihydrite. Such a mechanism was proposed earlier [50–52], and the results obtained in this

paper do not contradict the possibility of its implementation. The experimentally observed weakening of the impact of the cooling rate in the external field H_{FC} on the magnitude of the magnetization with the increase of H_{FC} does not contradict this mechanism, see Figure 1, *d*. The „antiferromagnetically similar" structure (Figure 3, *b*) will become energetically unfavourable with an increase of the external field. The value $\mu_P \cdot H$ in the field of 1 kOe is of the order 10 K (the magnetic moment of the particles is ~ 150 Boron magnetons [40]). In fact, if the Zeeman energy $\mu_P \cdot H$ becomes comparable to the energy of MII — E_{MII}, then the effects of the cooling rate in the external field H_{FC} on the magnitude of the magnetization will weaken.

On the other hand, if the MII in the system is significantly weakened, then there is no longer a factor affecting the rearrangement of the vectors μ_P against each other in case of cooling in the external field below the temperature T_B. On the contrary, the presence of an external field allows the magnetic moments μ_P to be fixed in the potential of magnetic anisotropy during the cooling process and preferably remain in the direction parallel to the external field. The above is a classical description of the processes of SPM blocking of non-interacting single-domain magnetic particles and explains the slight increase of magnetization (dependences $M_{FCC}(T)$ and $M_{FCW}(T)$) with the decrease of the temperature, see Figure 2. In this case, the cooling rate (at least in the range used $1-10$ K/min) no longer affects the magnetization.

4. Conclusions

A comparative study of the temperature dependences of the magnetization of two representative systems of ferrihydrite nanoparticles, in which either strong magnetic interparticle interactions are present or these interactions are weakened, revealed the following patterns. A significant effect of the cooling rate, at least in the range $\sim 1-10$ K/min, on the magnitude of the magnetization at low temperature is observed in the case of strong MII, if the system is cooled in an external field from a temperature exceeding the blocking temperature. As a result, the type of temperature dependence of the magnetization in case of sample heating $M_{FCW}(T)$ depends on the cooling rate. In addition, a significant difference between the temperature dependences of the magnetization in case of cooling $M_{FCC}(T)$ and in case of heating $M_{FCW}(T)$ of the sample is observed for a low cooling rate. These effects occur in weak fields (up to ~ 300 Oe), and they become weakly manifested with a further increase of the external field (up to 800 Oe). The effect of the cooling rate in the specified range $\sim 1-10$ K/min and the difference between the dependences $M_{FCC}(T)$ and $M_{FCW}(T)$ are insignificant for a sample in which the MII are weakened.

The revealed manifestation of MII in the magnetic properties of nanoferrihydrite is explained in the following scenario. The effect of the MII is such that it leads to a predominantly „antiferromagnetically similar" configuration of the magnetic moments of neighboring particles at temperatures below the SPM blocking temperature. The directions of the magnetic moments of the particles are rearranged during slow cooling from their preferred orientation along the external field (characteristic of the SPM state) to a structure in which the vectors of the magnetic moments of neighboring particles are predominantly directed against each other. An increase of the external field to such an extent that the Zeeman energy of the magnetic moment of the particle becomes comparable to the energy of the MII leads to a weakening of the impact of the MII and the destruction of the antiferromagnetic-like arrangement of the magnetic moments of the particles.

Acknowledgments

The authors are grateful to Yu.V. Knyazev for discussing the results.

Funding

The study was performed under the state assignment of the Institute of Physics, Siberian Branch of RAS.

Conflict of interest

The authors declare the absence of conflicts of interest.

References

[1] V.F. Cardoso, A. Francesko, C. Ribeiro, M. Bañobre-López, P. Martins, S. Lanceros-Mendez. Advanced Healthcare Materials **7**, *5*, 1700845 (2017).
[2] Z. Ma, J. Mohapatra, K. Wei, J. Ping Liu, S. Sun. Chem. Rev. **123**, 3904 (2023).
[3] M. Mohapatra, D. Hariprasad, L. Mohapatra, S. Anand, B. Mishra. Appl. Surf. Sci. **258**, *10*, 4228 (2012).
[4] F. Bødker, S. Mørup, S. Linderoth. Phys. Rev. Lett. **72**, 282 (1994).
[5] F.G. Silva, J. Depeyrot, Yu.L. Raikher, V.I. Stepanov, I.S. Poperechny, R. Aquino, G. Ballon, J. Geshev, E. Dubois, R. Perzynski. Scientific Reports **11**, 5474 (2021).
[6] D.A. Balaev, I.S. Poperechny, A.A. Krasikov, S.V. Semenov, S.I. Popkov, Y.V. Knyazev, V.L. Kirillov, S.S. Yakushkin, O.N. Martyanov, and Yu.L. Raikher. J. Phys. D: Appl. Phys. **54**, 275003 (2021).
[7] I.G. Vazhenina, R.S. Iskhakov, L.A. Chekanova. Physics of the Solid State, **60**, No 2, 292 (2018).
[8] A. Omelyanchik, M. Salvador, F. D'Orazio, V. Mameli, C. Cannas, D. Fiorani, A. Musinu, M. Rivas, V. Rodionova, G. Varvaro, D. Peddis. Nanomaterials **10**, 1288 (2020).
[9] D.A. Balaev, A.A. Dubrovsky, Yu.V. Knyazev, S.V. Semenov, V.L. Kirillov, O.N. Martianov. Physics of the Solid State **65**, No 6, 938 (2023).
[10] S. Mørup, D.E. Madsen, C. Fradsen, C.R.H. Bahl, M.F. Hansen. J. Phys.: Condens. Matter **19**, 213202 (2007).
[11] S. Mørup, M.F. Hansen, C. Frandsen. Beilstein J. Nanotechnol. **1**, 182 (2010).
[12] X. Batlle, C. Moya, M. Escoda-Torroellla, Ò. Iglesias, A.F. Rodríguez, A. Labarta. J. Magn. Magn. Mater. **543**, 168594 (2022).

[13] M. Knobel, W.C. Nunes, L.M. Socolovsky, E. De Biasi, J.M. Vargas, J.C. Denardin. Journal of Nanoscience and Nanotechnology **8**, 2836 (2008).
[14] V. Russier. J. Magn. Magn. Mater. **409**, 50 (2016).
[15] P.C. Rivas Rojas, P. Tancredi, O. Moscoso Londoño, M. Knobel, L.M. Socolovsky. J. Magn. Magn. Mater. **451**, 688 (2018).
[16] D.A. Balaev, S.V. Semenov, A.A. Dubrovskiy, S.S. Yakushkin, V.L. Kirillov, O.N. Martyanov. J. Magn. Magn. Mater. **440**, 199 (2017).
[17] H.T. Yang, D. Hasegawa, M. Takahashi, T. Ogawa. Appl. Phys. Lett. **94**, 013103 (2009).
[18] C.J. Bae, S. Angappane, J.-G. Park. Appl. Phys. Lett. **91**, 102502 (2007).
[19] C.A.M. Vieira, R. Cabreira Gomes, F.G. Silva, A.L. Dias, R. Aquino, A.F.C. Campos, J. Depeyrot. J. Phys.: Condens. Matter **31**, 175801 (2019).
[20] G.C. Papaefthymiou, E. Devlin, A. Simopoulos, D.K. Yi, S.N. Riduan, S.S. Lee, J.Y. Ying. Phys. Rev. B **80**, 024406 (2009).
[21] Yu.V. Knyazev, D.A. Balaev, S.V. Stolyar, A.A. Krasikov, O.A. Bayukov, M.N. Volochaev, R.N. Yaroslavtsev, V.P. Ladygina, D.A. Velikanov, R.S. Iskhakov. Journal of Alloys and Compounds **889**, 161623 (2021).
[22] D.A. Balaev, S.V. Stolyar, Yu.V. Knyazev, R.N. Yaroslavtsev, A.I. Pankrats, A.M. Vorotynov, A.A. Krasikov, D.A. Velikanov, O.A. Bayukov, V.P. Ladygina, R.S. Iskhakov. Results in Physics **35**, 105340 (2022).
[23] F. Fabris, K.-H. Tu, C.A. Ross, W.C. Nunes. J. Appl. Phys. **126**, 173905 (2019).
[24] S.V. Komogortsev, R.S. Iskhakov, V.A. Felk. J. Exp. Theor. Phys. **128**, 754 (2019).
[25] T. Raczka, A. Wolf, J. Reichstein, C. Stauch, B. Schug, S. Mússig, K. Mandel. Journal of Magnetism and Magnetic Materials **598**, 172042 (2024)
[26] O. Petracic. Superlattices and Microstructures **47**, 569 (2010).
[27] O. Petracic, X. Chen, S. Bedanta, W. Kleemann, S. Sahoo, S. Cardoso, P.P. Freitas. J. Magn. Magn. Mater. **300**, 192 (2006).
[28] K. Nadeem, H. Krenn, T. Traussnig, R.Wurschum, D.V. Szaboc, I. Letofsky-Papst. J. Magn. Magn. Mater. **323**, 1998 (2011).
[29] J.A. Ramos-Guivar, A.C. Krohling, E.O. Lopez, F.J. Litterst, E.C. Passamani. J. Magn. Magn. Mater. **485**, 142 (2019).
[30] M. Seehra, V.S. Babu, A. Manivannan. J. Lynn, Phys. Rev. B **61**, *5*, 3513−3518 (2000).
[31] N.J.O. Silva, V.S. Amaral, L.D. Carlos. Phys. Rev. B **71**, 184408 (2005).
[32] A. Punnoose, T. Phanthavady, M. Seehra, N. Shah, G. Huffman. Phys. Rev. B **69** (5), 054425 (2004).
[33] Ch. Rani, S.D. Tiwari. Physica B **513**, 58 (2017).
[34] C. Rani, S. Tiwari. Journ. Magn. Magn Mater. **385**, 272−276 (2015).
[35] C. Rani, S.D. Tiwari. J. Magn. Magn. Mater. **587**, 171341 (2023).
[36] S.I. Popkov, A.A. Krasikov, D.A. Velikanov, V.L. Kirillov, O.N. Martyanov, D.A. Balaev. J. Magn. Magn. Mater. **483**, 21 (2019).
[37] D.A. Balaev, A.A. Krasikov, S.I. Popkov, S.V. Semenov, M.N. Volochaev, D.A. Velikanov, V.L. Kirillov, O.N. Martyanov. Journal of Magnetism and Magnetic Materials **539**, 168343 (2021).
[38] T. Iimor, Y. Imamoto, N. Uchida, Y. Kikuchi, K. Honda, T. Iwahashi, Y. Ouch. J. Appl. Phys. **127**, 023902 (2020).
[39] A.A. Krasikov, D.A. Balaev. J. Exp. Theor. Phys **136**, No 1, pp. 97 (2023).
[40] A.A. Krasikov, D.A. Balaev, A.D. Balaev, S.V. Stolyar, R.N. Yaroslavtsev, R.S. Iskhakov. Journ. Magn. Magn. Mater. **592**, 171781 (2024).
[41] M. Tadic, D. Nikolic, M. Panjan, G.R. Blake. Journal of Alloys and Compounds **647**, 1061 (2015).
[42] E. Winkler, R.D. Zysler, D. Fiorani. Phys. Rev. B **70**, 174406 (2004).
[43] C. Frandsen, S. Mørup. Phys. Rev. Lett. **94**, 027202 (2005).
[44] C. Frandsen, C.W. Ostenfeld, M. Xu, C.S. Jacobsen, L. Keller, K. Lefmann, S. Mørup. Phys. Rev. B **70**, 134416 (2004).
[45] E.L. Duarte, R. Itri, E. Lima Jr, M.S. Baptista, T.S. Berqu'o, G.F. Goya. Nanotechnology **17**, 5549 (2006).
[46] T.S. Berquó, J.J. Erbs, A. Lindquist, R.L. Penn, S.K. Banerjee. J. Phys.: Condens. Matter **21**, 176005 (2009).
[47] Yu.V. Knyazev, D.A. Balaev, R.N. Yaroslavtsev, A.A. Krasikov, D.A. Velikanov, Yu.L. Mikhlin, M.N. Volochaev, O.A. Bayukov, S.V. Stolyar, R.S. Iskhakov. Advances in Nano Research **12**, 605 (2022).
[48] Yu.V. Knyazev, D.A. Balaev, S.A. Skorobogatov, D.A. Velikanov, O.A. Bayukov, S.V. Stolyar, V.P. Ladygina, A.A. Krasikov, R.S. Iskhakov. Physics of Metals and Metallography **125**, *4*, 377 (2024).
[49] Yu.V. Knyazev, D.A. Balaev, S.A. Skorobogatov, D.A. Velikanov, O.A. Bayukov, S.V. Stolyar, R.N. Yaroslavtsev, R.S. Iskhakov. Phys. Rev. B **107**, 115413 (2023).
[50] D.A. Balaev, A.A. Krasikov, Y.V. Knyazev, R.N. Yaroslavtsev, D.A. Velikanov, Y.L. Mikhlin, M.N. Volochaev, O.A. Bayukov, V.P. Ladygina, S.V. Stolyar, R.S. Iskhakov. Nano-Structures & Nano-Objects **37**, 101089 (2024).
[51] A.A. Krasikov, Yu.V. Knyazev, D.A. Balaev, S.V. Stolyar, V.P. Ladygina, A.D. Balaev, R.S. Iskhakov. J. Exp. Theor. Phys. **137**, (N 6), 903 (2023).
[52] A.A. Krasikov, Yu.V. Knyazev, D.A. Balaev, D.A. Velikanov, S.V. Stolyar, Yu.L. Mikhlin, R.N. Yaroslavtsev, R.S. Iskhakov. Physica B **660**, 414301 (2023).
[53] M. Knobel, W.C. Nunes, H. Winnischofer, T.C.R. Rocha, L.M. Socolovsky, C.L. Mayorga, D. Zanchet. Journal of Non-Crystalline Solids **353**, 743 (2007).
[54] D.A. Velikanov. Vestnik SibGAU **14**, *2*, 176 (2013). (in Russian).
[55] A.D. Balaev, Yu.V. Boyarshinov, M.M. Karpenko, B.P. Khrustalev. Instrum. Exp. Tech. (Engl. Transl.) **26** (3) [Prib. Tekh. Eksp. **3**, 167 (1985)].
[56] N.J.O. Silva, V.S. Amaral, A. Urtizberea, R. Bustamante, A. Millan, F. Palacio, E. Kampert, U. Zeitler, S. de Brion, O. Iglesias, A. Labarta. Phys. Rev. B **84**, 104427 (2011).
[57] D.A. Balaev, A.A. Krasikov, A.D. Balaev, S.V. Stolyar, V.P. Ladygina, R.S. Iskhakov. Physics of the Solid State **62**, 1172–1178 (2020).
[58] F. Luis, E. del Barco, J.M. Hernandez, E. Remiro, J. Bartolome, J. Tejada. Phys. Rev. B **59**, 11838 (1999).
[59] M. Suzuki, S.I. Fullem, I.S. Suzuki, L. Wang, Ch.-J. Zhong. Phys. Rev. B **79**, 024418 (2009).
[60] K. Konwar, S.D. Kaushik, D. Sen, P. Deb. Phys. Rev. B **102**, 174449 (2020).
[61] M. Sasaki, P.E. Jönsson, H. Takayama, H. Mamiya. Phys. Rev. B **71**, 104405 (2005).
[62] J.A. De Toro, P.S. Normile, S.S. Lee, D. Salazar, J. Liang Cheong, P. Munñiz, J.M. Riveiro, M. Hillenkamp, F. Tournus, A. Tamion, P. Nordblad. J. Phys. Chem. C **117**, 10213 (2013).

Translated by A.Akhtyamov